Features of Designing Control Systems of Tested Aviation Moving Platforms

Olha Sushchenko[1], Yurii Bezkorovainyi[1(✉)], Oleksandr Solomentsev[1], Maksym Zaliskyi[1], Oleksii Holubnychyi[1], Ivan Ostroumov[1], Yuliya Averyanova[1], Viktoriia Ivannikova[1], Borys Kuznetsov[2], Ihor Bovdui[2], Tatyana Nikitina[3], Roman Voliansky[4], Kostiantyn Cherednichenko[1], and Olena Sokolova[1]

[1] State University "Kyiv Aviation Institute", Liubomyra Huzara Avenue, 1, Kyiv 03058, Ukraine
yurii.bezkor@gmail.com

[2] Anatolii Pidhornyi Institute of Mechanical Engineering Problems of the National Academy of Sciences of Ukraine, Pozhars'koho Street, 2/10, Kharkiv 61046, Ukraine

[3] Educational Scientific Professional Pedagogical Institute Ukrainian Engineering Pedagogical Academy, University Street 16, Kharkiv 61003, Ukraine

[4] National Technical University of Ukraine "Igor Sikorsky Kyiv Polytechnic Institute", Beresteiskyi Avenue, 37, Kyiv 03056, Ukraine

Abstract. This paper describes the features of designing control systems for moving platforms with equipment of different types including optical sensors, antennas, video cameras, and observation equipment. The features of linearization of the mathematical description are described. Such features include the influence of the hysteresis in the gyroscopic device and the backlash in the controlling drive of the platform. The recommendations for linearization of the non-linearities as mentioned earlier are given. The features of introducing disturbances in the mathematical description of moving platforms are represented. The technique of creating forming filters for the simulation of disturbances caused by irregularities of relief of road and terrain is described. Such an approach is relevant for moving platforms operated on land vehicles. The procedure for creating a robust controller resistant to internal and external disturbances is given. The synthesis of the control system for the moving platform has been realized. The simulation results are represented. The obtained results can be useful for the control systems of the different moving vehicles.

Keywords: Land Vehicle · Motion Control · Stabilization System · Linearization · Forming Filters · Disturbances · Simulation

1 Introduction

Currently, the relevance of improving existing and creating high-precision control systems for payloads intended for use on aviation-tested moving platforms is increasing. The solution to this problem requires using inertial stabilized platforms that, in turn, leads to the need to create systems for their control [1–3].

© The Author(s), under exclusive license to Springer Nature Switzerland AG 2026
O. Gervasi et al. (Eds.): ICCSA 2025 Workshops, LNCS 15888, pp. 140–151, 2026.
https://doi.org/10.1007/978-3-031-97596-7_9

The typical tasks of control of payloads operated on aviation-tested moving platforms include the following items.

1. Stabilization of the payload in the vertical and horizontal planes during angular movement of the object.
2. Guidance of the payload sighting axis to fixed and moving reference points.
3. Combination of the first two modes, i.e. stabilized guidance of the payload sighting axis to the reference point.

It is worth mentioning that two-axis stabilization is generally relevant for payloads installed on ground-based mobile objects. In most cases, horizontal and vertical stabilization can be considered separately [4–6].

The purpose of this research is to study features of designing systems for the control of moving platforms assigned for the operation of vehicles. The moving platforms are used for stabilization of different payloads including optical sensors, antennas, and different equipment.

In the paper, such important features of designing motion control systems as linearization and introducing stochastic disturbances are considered. The efficiency of system synthesis is proved by modelling. It is worth mentioning that problems of the developing models of the considered class of systems were studied in detail in the paper [7]. The represented results and mathematical models described in [7] allow us to carry out the synthesis of the control system with good efficiency.

The paper's structure looks in the following way. Section 2 deals with features of the linearization of the theoretical representation of the considered system. The features of introducing stochastic disturbances mathematically are given in Sect. 3. The numerical demonstration of the results of the synthesized system is shown in Sect. 4.

2 Features of Linearization

The significance of developing improved perspective systems for controlling aviation-tested mobile platforms has recently been growing. The development of the mentioned systems requires the research of techniques for synthesis and analysis, which could ensure the successful production of improved researched system specimens. A well-known software tool of this type is the Control Toolbox containing a significant set of procedures for designing perspective control systems. However, the features of such a toolbox include its operation only with linear time-invariant models. At the same time, real stabilization systems are usually non-linear, so there is a need to analyze typical non-linearities and the possibilities of transition to a linearized model [8–10].

A mathematical model of a stabilization system for a land-based object is a set of mathematical models of devices included in this system. Before the main devices, there are a gyro device, electronic devices, and motors.

The change in the absolute velocity of a tested aviation moving platform can be measured using an additional gyro device. The mathematical description of the gyro device in terms of the output rotation angle and voltage becomes [11]:

$$\begin{gathered} J_g\ddot{\alpha} + 2\nu\sqrt{J_g c_t}\dot{\alpha} + M_\alpha - M_{gt}^1 + M_{gt}^2 - M_{fr} = M_{im} - \dot{\omega}_\eta J_g; \\ \ddot{U} = k_{adt}\alpha + U_0, \end{gathered} \tag{1}$$

here J_g is the torque of inertia of gyro device gimbals; ν is the damping coefficient; c_t is torsion rigidity; M_α is the moment taking into account the torsion's hysteresis; $M_{gt}^1 = S\omega_\xi \cos\alpha$ is the gyroscopic moment caused by the influence of measured angular rate ω_ξ, here S is the kinetic moment of the gyroscopic device; $M_{gt}^2 = S\omega_\zeta \sin\alpha$ is the gyroscopic moment due to the action of the angle rate ω_ζ perpendicular to the measured one; $M_{fr} = -M_f \operatorname{sign}\dot{\alpha}$ is the friction torque in gimbals bearings; $M_{im} = \delta W$ is the moment of imbalance, here δ is the displacement due to imbalance; W is acceleration, which leads to imbalance; $\dot{\omega}_\eta$ is the angle acceleration along to the longitudinal axis of the gyro device; k_{adt} is the transfer factor of the angle data transmitter; U_0 is the zero shift of the angle sensor.

The main nonlinearity in the model of the gyro device arises due to the necessity to regulate the influx of torsion bar hysteresis. This method is used to formulate a moment consistent with such an algorithm.

As soon as the condition $\dot{\alpha} \le 0$ is finalized, then the moment $\boldsymbol{M_\alpha}$, depending on the range of vibrations, is formed in this way:

$$\begin{cases} M_\alpha = c_t\alpha_0, \text{ if } \alpha_0 - k_{gis}\alpha_0 \le \alpha \le \alpha_0; \\ M_\alpha = c_t\alpha, \quad \text{if } \alpha \le \alpha_0\left(1 - k_{gis}\right), \end{cases}) \tag{2}$$

where k_{gis} is the transfer coefficient, which characterizes the hysteresis value.

As soon as the condition $\dot{\alpha} > 0$ comes to an end, the moment M_α lies within the range of extinction and is designated as follows:

$$\begin{cases} M_\alpha = c_t\alpha_0, \text{ if } \alpha_0 \le \alpha \le \alpha_0 + k_{gis}\alpha_0; \\ M_\alpha = c_t\alpha, \quad \text{if } \alpha < \alpha_0\left(1 + k_{gis}\right). \end{cases} \tag{3}$$

The expressions (1) – (3) allow us to use the mathematical description of the gyro device with the non-linearity due to the hysteresis providing the qualitative synthesis of the system for control of the moving platform.

The next essential non-linearity of the stabilization system is caused by the backlash of the drive.

Manner is that the system of the considered type is assigned for stabilization of the equipment of large mass. In this case, the drive consists of a motor with great rotational speed and the reducer. Therefore, the effect of the backlash of the united system consisting of the stabilization object (platform with payload) and drive with the reducer has arisen [12–14].

The mathematical description of the stabilization object can be described in the form of a second-order differential equation [15]:

$$\mathrm{J_a}\ddot{\varphi}_\mathrm{a} + \mathrm{M_{fr}}\operatorname{sign}\dot{\varphi}_\mathrm{a} - \mathrm{M_{im}}\sin\varphi_\mathrm{a} + \mathrm{k_s}\varphi_\mathrm{a} + \mathrm{c_r}\varphi_\mathrm{a} = \mathrm{k_s A} + \frac{\mathrm{c_r}\varphi_\mathrm{b}}{\mathrm{n_r}} - \mathrm{M_{im}}, \tag{4}$$

where M_{fr} is the torque moment; M_{im} is the imbalance torque; k_s is the spring rigidity; A is an angle of the spring's deviation; J_a is the inertia torque; φ_a is the angle of rotation of the stabilization object.

The main non-linearities in the expression (4) are related to the moments of rubbing. They can be approximated by linear expressions represented in [16].

In this case, for the designated moment of rubbing $M = M_{fr}\text{sign}\dot{\varphi}_a$, it is replaced with linear constituent $M = f_a\dot{\varphi}_a$. At this rate, the coefficients f_a will appear as $f_a = 4M_{fr}/(\pi\Omega_a)$.

The flow chart of the modelling process for motor rotation due to non-linearity, resulting in engine backlash, is shown in Fig. 1.

Results of the simulation of the non-linearity due to backlash are described in Figs. 2 and 3.

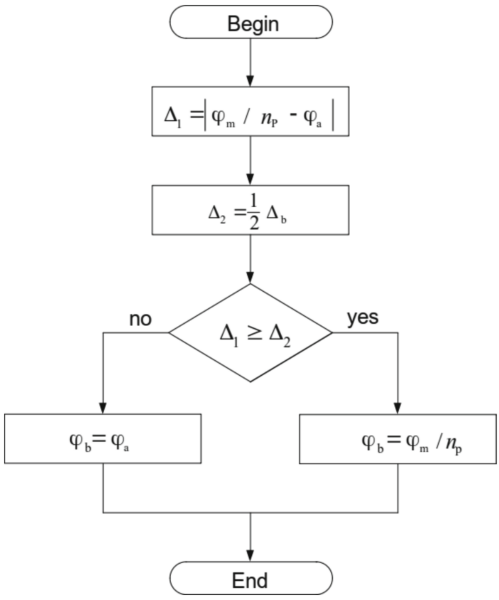

Fig. 1. Flow chart of the molding of the rotation of the motor taking into account the motor backlash due to inherent non-linearities (Δ_b. – backlash zone).

To confirm the obtained results, the horizontal channel of the system of stabilization of an aviation-tested moving platform was modeled. The presented results allow us to conclude the possibility of linearizing the model of the studied stabilization system [17–19].

Figures 2 and 3 illustrate the influence of the engine backlash (0.006 rad) on the transient processes of the angular velocity of an aviation-tested moving platform in the guidance mode. Typical nonlinearities of the studied model should also include the need to limit signals, which is easily implemented by Simulink tools. When dealing with such nonlinearities, it is recommended to work with relatively small values when using a linearized model. The most typical nonlinearities include the presence of insensitivity zones in real equipment, which cannot be taken into account in state space models. The corresponding modeling showed the appropriate transient processes. The simulation results also showed that neglecting such typical nonlinearities does not lead to a significant deterioration of the quality indices by the nonlinear component of the unbalanced moment for angles of rotation of the payload within 5–10 degrees.

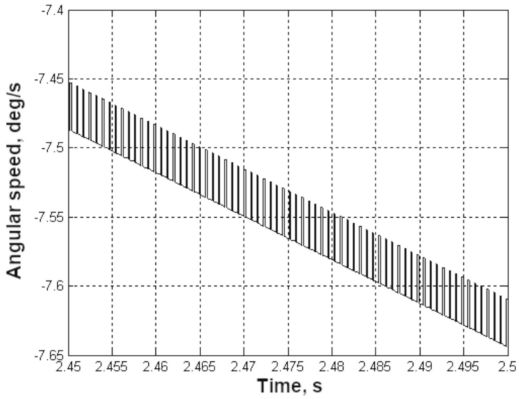

Fig. 2. The non-linearity due to backlash 0.006 rad.

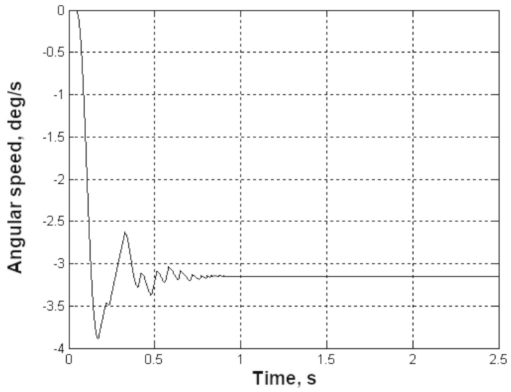

Fig. 3. Influence of the backlash on the transient process of the angular rate.

3 Features of Introducing External Disturbances

It is essential to perform the design procedure for the researched system using operating perturbations. For aviation-tested moving platforms, the disturbed action depends on the action roughnesses caused by the relief profile. For its part, the influence of relief roughnesses depends on terrain topographic features. Therefore, the simulation technique is based on the usage of roughnesses profile. This characteristic is defined by a section of the relief by the vehicle's motion direction [20–22].

For example, such specified relief as terrain with bumps can be expressed in random variables depending on bump altitudes. These random variables are connected also with length, i.e. the distance traveled, or the time. Random variables of this kind could be applied in studying the disturbed motion.

It is worth mentioning that in scientific and technical literature, distance functions are given. Nevertheless, this approach does not disagree with the earlier mentioned proposal as random variables can be expressed in distances using definite relationships.

In frequent situations, we could change the profile by the microprofile when determining random external movements. The specific feature of the microprofile is connected with the absence of constituents with low frequency.

The basic excellence of such a representation can be explained by the possibility of representing microprofile in the form of a random time-invariant process. Namely, such representation can be efficiently applied in procedures of analysis and synthesis of systems for controlling mobile platforms. The transformation of the profile $h(t)$ into microprofile $q(t)$ can be implemented by the fractional-rational transfer function H_q [23, 24].

As both profile and microprofile can be described by random processes, it is appropriate to apply them in procedures of the analysis and synthesis of spectral densities of these processes. These characteristics in dependencies of distance and time $q(l)$, $h(l)$ can be represented by the relations [24].

$$K_l(\lambda) = vK_l(\lambda v);\ K_l(\omega) = \frac{1}{v}K_l\frac{\omega}{v}. \tag{5}$$

The spectral density of the microprofile looks like

$$K_q(\omega) = \left|H_q(\omega)\right|^2 K_h(\omega), \tag{6}$$

where $H_q(\omega)$ is the transfer function of microprofile conversion

$$H_q(\omega) = \frac{(j\omega)^2}{(j\omega)^2 + \sqrt{2}\omega_n j\omega + \omega_n^2}. \tag{7}$$

In the simplified form, the expression (7) becomes

$$H_q(\omega) = \frac{j\omega}{j\omega + \omega_n}. \tag{8}$$

The classification of the spectral densities of the profile of roads and terrain is performed depending on the short roughnesses heights of the microprofile (6). At the same time, based on (5), (6), (8) and considering the length of the wave, we can divide relief rougnesses into three groups, which can be represented by the relationships [24]:

$$K(\lambda) = \frac{D_m}{\lambda^2};\ K(\lambda) = \frac{D_c}{\lambda^n};\ 0 \le n \le 4;\ K(\lambda) = \frac{D_n}{\lambda^2}. \tag{9}$$

The relationships (9) include factors D_m, D_c, D_n that describe the type and characteristics of the terrain relief. Every group of roughnesses is divided into some subgroups. These subgroups differ in various values of earlier mentioned factors:

- $D_m = 10^{-1}$ defines very rugged terrain with rolling hills;
- $D_c = 10^{-2}$, n = 2 corresponds to a field or meadowland characterizing high roughnesses and nearly equal influence of long and short waves;
- $D_n = 3 \bullet 10^{-3}$ corresponds to the terrain with inhomogeneous land, arable land, and stony ground.

Another way of roughnesses classification foresees four subgroups including prevalence of long unevennesses, bottom land, bulges, and uniform roughnesses. The spectral density for every subgroup is described by the following relationships.

- $K(\lambda) = \frac{D_2(3.1^2+\lambda^2)}{\lambda^2(\lambda_2^2+\lambda^2)}$ (five groups, the fifth group corresponds to very cross terrain $D_2 = 10^{-2}$, $\lambda_2 = 1$);
- $K(\lambda) = \frac{D_2(10+\lambda^2)(\lambda_1^2+\lambda^2)}{\lambda^2(1+\lambda^2)}$ (five groups, for the fourth group corresponds to large shafts $D_2 = 3.16 \bullet 10^{-3}$, $\lambda_1 = 0.178$);
- $K(\lambda) = \frac{D_2(\lambda_1^2+\lambda^2)}{\lambda^2(10^2+\lambda^2)}$ (six groups, the fifth group corresponds to large ramparts $D_2 = 10^{-1}$ $\lambda_1 = 1$;
- $(\lambda) = \frac{D_2}{\lambda^2}$ (five groups, the fourth group corresponds to the spectral density of a the high level $D_2 = 10^{-2}$).

Both the first and second classifications could be applied to the simulation of mobile platform motion accompanied by terrain roughnesses. It is worth mentioning that namely the second classification is the most suitable for simulating motion of considered mobile platforms. As the relief microprofile can be described by a normal random process. To imitate this process, we must set the white noise $\delta(t)$ at the input of forming filter with the transfer function H_m.

To design the forming filter, we must take into account the condition [24]

$$H_m(j\omega)H_m^*(j\omega) = K_\delta^{-1}K_q(\omega). \tag{10}$$

According to the second classification, the creation of forming filters has been implemented in the following way:

- $K_h(j\omega) = \frac{\sqrt{D_2 v}}{j\omega}\frac{(3.1v+j\omega)}{(v\lambda_2+j\omega)}$;
- $K_h(j\omega) = \frac{\sqrt{D_2 v}}{j\omega}\frac{(10v+j\omega)(v\lambda_1+j\omega)}{(v+j\omega)(v+j\omega)}$;
- $K_h(j\omega) = \frac{\sqrt{D_2 v}}{j\omega}\frac{(v\lambda_1+j\omega)}{(10v+j\omega)}$;
- $K_h(j\omega) = \frac{\sqrt{D_2 v}}{j\omega}$.

Finally, the expression for the representation of forming filters looks like

$$K_q(\omega) = K_h(j\omega)H_q(j\omega), \tag{11}$$

where $H_q(j\omega)$ is the transfer function of the microprofile conversion.

To synthesize the stabilization system of considered mobile platforms, it is desired to accept some definite kind of contact between the terrain and tires. This assumption must be supplemented by requirements for the kind of profile. The considered problem requires using a smoothed profile for simulation of the disturbed motion. It is characterized by averaging in the contact area. The transfer response of the averaged contact area corresponds to wheel smoothing possibility. Nearly, it can be given in the following representation [24]

$$H_k(\omega) = \frac{\omega_b^2}{(j\omega)^2 + \sqrt{2}\omega_d j\omega + \omega_b^2}, \tag{12}$$

The expression (12) can be represented in the simplified form

$$H_k(\omega) \approx \frac{\omega_b}{j\omega + \omega_b}, \tag{13}$$

where $\omega_b(0.9 - 1.3)v/a$; v is the velocity of the mobile platform, a is the width of a contacting area.

In order to take into account the disturbances acting on the system, it is necessary to consider the serial connection of the system model and the forming filter based on expressions (10), (11), and (13).

The process of stabilizing the spatial position of a moving platform under the condition of the test signal and under the condition of the disturbance is shown in Figs. 4 and 5, where the stabilized spatial location of the platform in conditions of the tested signal and simulated disturbances are represented.

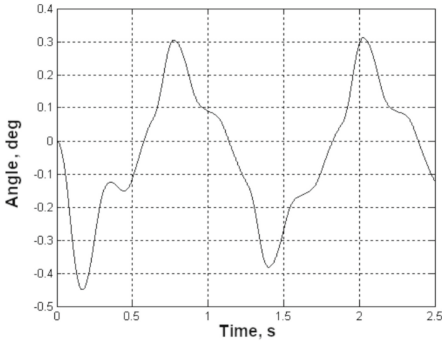

Fig. 4. Stabilization of the platform in conditions of the tested signal.

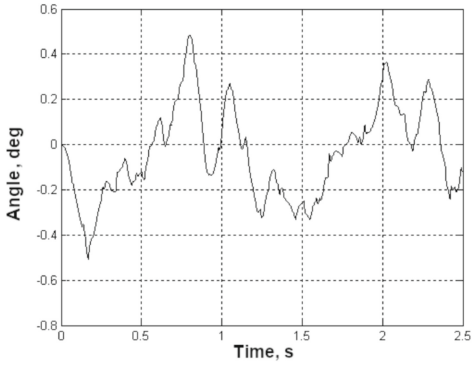

Fig. 5. Stabilization of the platform in conditions of the disturbed signal.

4 Design of the System for Motion Control and Modelling Results

The block diagram of the algorithm for the stabilization system synthesis is presented in Fig. 6.

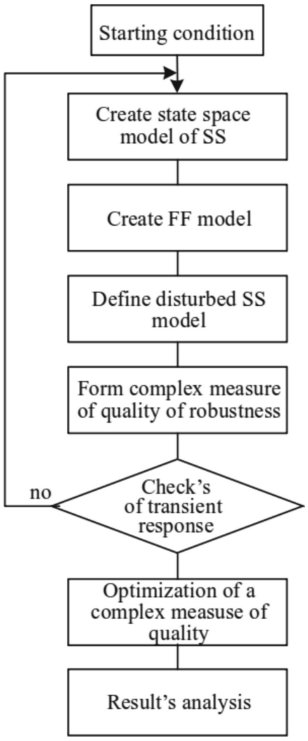

Fig. 6. Flow chart of the procedure for the synthesis of the control system for moving platform: SS is the stabilization system, FF is the forming filter.

The synthesis procedure is grounded on an objective function that considers the most important feature of the designed system. For the considered systems, the most preferred is applying the combined optimization function taking into account the quality and robustness. Such an approach ensures both the accuracy of the system and its resistance to internal and external disturbances. Namely, these properties are of great importance for control systems of mobile platforms. Separate constituents of the objective function have been created using H_2, $H_\infty-$ norms [25]. The H_2-norm represents the square root of the averaging impulse response. This constituent could be expressed as the output signal power in the system's stable state under the influence of the white noise with the unit intensity. The $H_\infty-$ norm represents the maximum of the system's frequency response. The influence of every constituent in the combined objective function is defined by weight coefficients. These coefficients are defined by requirements to the system [26]. Modelling results are represented in Figs. 7 and 8.

The synthesized system is characterized by amplitude stability margins of 53.3 dB and phase 91.2 degrees, values of accuracy and robustness $H_2 = 0.3736$ and $H_\infty = 0.1177$, and angular stiffness of 175 Nm/arcmin. Given this, the proposed procedure of the synthesis of considered systems simultaneously takes into account the quality and robustness [27–29]. The proposed synthesis procedure has been implemented with the help of Nelder-Mead method. The controller of the system has been created on the basis

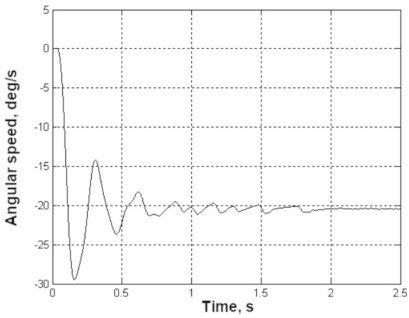

Fig. 7. The transient process on the angular rate for the terrain with middle roughnesses.

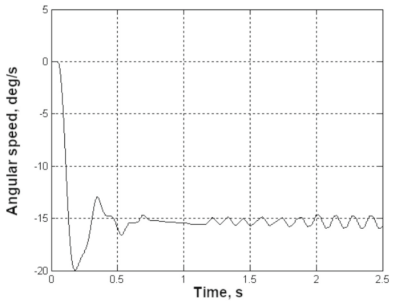

Fig. 8. The transient process on the angular rate for the terrain with bumps.

of the robust structural synthesis. The designed controller is grounded on the feedback by an angular rate of the platform [30]. The structure of the robust controller is automatically obtained as a result of the procedure of the robust structural synthesis. It is represented in the form of a quadruple of state-space matrices of the sixth order and is not given here for simplicity. On the whole, it represents PID controller with additional components caused by specific features of the mobile platform.

5 Conclusions

Approaches to linearization of the mathematical description and simulation disturbances arising due to terrain relief roughnesses using forming filters are considered. The flow chart of the procedure for the synthesis of a control system for the mobile platform is presented. The features of linearization for the control system of mobile platforms are explained.

The procedure of the synthesis of the considered system is represented. The proposed procedure is grounded on the combined objective function including accuracy and robustness of the system.

The obtained simulation results prove the efficiency of the proposed synthesis procedure. This is shown by the transient processes of the mobile platform motion in normal and disturbed conditions.

It is planned during future research to carry out similar research relative to unmanned aerial vehicles. The approach to introducing disturbances in the mathematical description of the moving platforms for equipment operated on unmanned aerial vehicles is planned.

References

1. Hilkert, J.M.: Inertially stabilized platform technology. IEEE Control. Syst. Mag. **1**, 26–46 (2008)
2. Masten, M.K.: Inertially stabilized platforms for optical imaging systems. IEEE Control. Syst. Mag. **1**, 47–64 (2008)
3. Ostroumov, I., Kuzmenko, N., Bezkorovainyi, Y., Averyanova, Y., Larin, V., et al.: Relative navigation for vehicle formation movement. In: 3rd KhPI Week on Advanced Technology, pp. 1–4. IEEE, Kharkiv, Ukraine (2022). https://doi.org/10.1109/KhPIWeek57572.2022.9916414
4. Zoppoli, R., Sanguineti, M., Gnecco, G., Parisini, T.: Neural Approximations for Optimal Control and Decision. Springer, Cham (2020)
5. Osadchy, S.I., Zozulya, V.A., Bereziuk, I.A., Melnichenko, M.M.: Stabilization of the angular position of hexapod platform on board of a ship in the conditions of motions. Autom. Control. Comput. Sci. **56**(3), 221–229 (2022)
6. Bittanti, S.: Model Identification and Data Analysis. John Wiley & Sons, New Jersey (2019)
7. Sushchenko, O., Bezkorovainyi, Y., Salyuk, O., Yehorov, S.: Mathematical description of system for stabilization of aviation equipment in problems of synthesis and simulation. In: Ostroumov, I., Zaliskyi, M. (eds.) Proceedings of the 2nd International Workshop on Advances in Civil Aviation Systems Development. ACASD 2024, Lecture Notes in Networks and Systems, vol. 992, pp. 73–85. Springer, Cham (2024). https://doi.org/10.1007/978-3-031-60196-5_7
8. Sushchenko, O.A., Shyrokyi, O.V.: H2/H∞ optimization of system for stabilization and control by line-of-sight orientation of devices operated at UAV. In: IEEE 3rd International Conference Actual Problems of Unmanned Aerial Vehicles Developments (APUAVD), pp. 235–238. IEEE, Kyiv, Ukraine (2015). https://doi.org/10.1109/APUAVD.2015.7346608
9. Fu, J., Ma, R.: Stabilization and Hinf Control of Switched Dynamic Systems. Springer, Berlin (2020)
10. Kuznetsov, B.I., Nikitina, T.B., Bovdui, I.V.: Structural-parametric synthesis of rolling mills multi-motor electric drives. Electr. Eng. Electromechanics **5**, 25–30 (2020). https://doi.org/10.20998/2074-272X.2020.5.04
11. Zhuang, X., Li, P., Li, D., Sui, W.: Gyroscopes – Principles and Applications. IntechOpen, London (2020)
12. Hernandez-Gurman, V.M., Silva-Ortigoza, R.: Automatic Control with Experiments. Springer, Berlin (2019)
13. Zerrik, El. H., Castillo O.: Stabilization of Infinite Dimensional Systems. Springer, Cham (2021)
14. Kuznetsov, B.I., Nikitina, T.B., Bovdui, I.V.: Multiobjective synthesis of two degree of freedom nonlinear robust control by discrete continuous plant. Tech. Electrodynamics **5**, 10–14 (2020). https://doi.org/10.15407/techned2020.05.010
15. Niu, S.S., Xiao, D.: Process Control: Engineering Analysis and Best Practices. Springer, New York (2022)
16. Sanfelice, R.G.: Hybrid Feedback Control. Princeton University Press, Princeton (2021)
17. Wang, L.: PID Control System Design and Automatic Tuning using MATLAB/Simulink. Wiley, Hoboken (2020)

18. Le, A.T.: Adaptive Robust Control Systems. Intech Open, Vienna (2018)
19. Osadchyi S., Zozulia, V.: Synthesis of optimal multivariable robust systems of stochastic stabilization of moving objects. In: 5th International Conference Actual Problems of Unmanned Aerial Vehicles Developments (APUAVD), pp. 106–111. IEEE, Kyiv, Ukraine (2019). https://doi.org/10.1109/APUAVD47061.2019.8943861
20. Wright, S.J., Recht, B.: Optimization for Data Analysis. Cambridge University Press, Cambridge (2022)
21. Lia, Y., Huang, N.Z., Jiang, T.: Selective Maintenance Modelling and Optimization. Springer, Cham (2023)
22. Khachaturov, A.A.: Dynamics of system road-tyre–car–driver. https://h.twirpx.link/file/570103/
23. Popp, K., Schiehlen, W.: Ground Vehicle Dynamics. Springer, Berlin (2010)
24. Scogestad, S., Postlathwaite, I.: Multivariable Feedback Control. Analysis and Design. John Wiley & Sons, London (2005)
25. Asadi, F.: State-Space Control Systems: The MATLAB/Simulink Approach. Morgan & Claypool, Sun Rafael (2021)
26. Zhiteckii, L.S., Azarskov, V.N., Solovchuk, K.Y., Sushchenko, O.A.: Discrete-time robust steady-state control of nonlinear multivariable systems: a unified approach. IFAC Proc. Volumes **47**(3), 8140–8145 (2014). https://doi.org/10.3182/20140824-6-ZA-1003.01985
27. Voliansky, R., Sadovoi, A., Volianska, N.: Interval model of the piezoelectric drive. In: 14th International Conference on Advanced Trends in Radioelecrtronics, Telecommunications and Computer Engineering (TCSET), pp. 1–6, IEEE, Lviv-Slavske, Ukraine (2018). https://doi.org/10.1109/TCSET.2018.8336211
28. Niu, S.S., Xiao, D.: Process Control. Springer, Berlin (2022)
29. Sushchenko, O.A., Bezkorovainyi, Y.N., Novytska, N.D.: Dynamic analysis of nonorthogonal redundant inertial measuring units based on MEMS-sensors. In: 38th International Conference on Electronics and Nanotechnology, ELNANO-2018, pp. 464–469. IEEE, Kyiv, Ukraine (2018). https://doi.org/10.1109/ELNANO.2018.8477553
30. Chikovani, V., Sushchenko, O., Tsiruk, H.: Redundant information processing techniques comparison for differential vibratory gyroscope. Eastern Eur. J. Enterp. Technol. **4**(7), 45–52 (2016). https://doi.org/10.15587/1729-4061.2016.75206